

# Off-axis transmission holographic system for recording aquatic particles

E. P. Krantz<sup>a</sup>, J. Watson<sup>a</sup>, P. R. Hobson<sup>b</sup>, R. S. Lampitt<sup>c</sup>, A. Rogerson<sup>d</sup>

<sup>a</sup>Department of Engineering, Kings College, University of Aberdeen, Aberdeen, Scotland

<sup>b</sup>Department of Physics, Brunel University, Uxbridge, England

<sup>c</sup>Southampton Oceanography Centre, Empress Dock, Southampton, England

<sup>d</sup>University Marine Biological Station Millport, Isle of Cumbrae, Scotland

## ABSTRACT

We describe a holographic system for recording particles suspended in water. The hologram plate is located in air, separated from the test tank by an air/glass/water boundary. The holographic emulsion is therefore unaffected by adverse aquatic conditions within the tank (i.e. surface contamination, non-uniform swelling). The design geometry is intended to minimise the aberrations that arise from recording subjects located in water and replaying their hologram image in air. Third order aberrations, most crucially spherical aberration and astigmatism, are suppressed to give an experimental resolution of 7 lp/mm using USAF 1951 target in water 600 mm from the boundary. Particles (plankton species) in the sub-millimeter to several millimeters size range are observed at planar sections within the recording volume by visual inspection of the hologram replayed in real image mode.

**Keywords:** holographic, holography, aquatic, particle

## 1. INTRODUCTION

There is substantial interest in obtaining data that leads scientists to better understand the interactions of particles in the aquatic environment<sup>1-5</sup>. The conventional methods of gathering data on aquatic particles of both living and non-living material are not well suited to observing their precise spatial location within a large volume. For example, electronic counting techniques tend to damage particles and to disrupt their spatial position. Another example is conventional photography, which records a relatively shallow depth-of-field per exposure. Hence, sampling a large volume takes a considerable time, during which the distribution of particles may change. Laser (non-holographic) counting and sizing techniques have recently been applied *in situ* to particles (platelet aggregates) on the order of microns, but without spatial information<sup>6</sup>.

Holography is unique in the respect of recording a volume non-destructively while preserving the accurate spatial distribution of individual particles<sup>7</sup>. Moreover, a pulsed hologram can capture the entire volume in a single 40 ns exposure and sequential holograms can record changes within the volume over time. The particles can be systematically examined by interrogating their real image using a CCD camera or microscope mounted on a computer controlled micropositioner. In-line holography has been successful in the recording and replay of aquatic particles on the order of tens of microns in size<sup>8,9</sup>. Recent work has produced identifiable images of plankton species and spatial co-ordinates precise to  $\pm 5$  microns<sup>10</sup>. However, in-line Fraunhofer holography can not cope with particles larger than approximately one millimetre.

Whereas the size and population densities of particles can be predicted for in-line holographic image formation (based on satisfying approximately 80% transmittance of the beam and the far-field conditions), there is no general prediction that is applicable to the entire range of off-axis configurations. This is because variations of illumination and reference beam geometries can produce varying results. For example, one off-axis set-up may fail to record sub-millimetre sized particles (i.e.. due to insufficient irradiance at the recording plate) where another may succeed. Hence, the characteristics, or morphology, of the particle subjects (e.g. size, reflectivity<sup>11</sup>) are integral to the success of an off-axis configuration<sup>12</sup>.

We describe an off-axis transmission holographic system for recording aquatic particles that surpasses the upper bounds of in-line holography in terms of subject size and population density. For practical purposes, the hologram plate is located in air, separated from the aquatic test tank by an air/glass/water boundary. This design introduces a refractive index mismatch between the holographic recording of subjects in water and image reconstruction in air. The mismatch gives rise to aberrations that degrade image fidelity<sup>13</sup>.

Our objectives are to construct a system that can record relatively small particles (sub-millimetre to several millimetre range) within a relatively large volume (greater than 3,000 cm<sup>3</sup>). Furthermore, image fidelity must meet acceptable tolerances. For our application, this means simply that individual particle images be positively identified (for example, in the case of plankton, by species). Moreover, we consider design options that are practical for the ultimate implementation of the system in the field. In the sections that follow we describe the design parameters and the design decisions that lead to the construction of our experimental set-up. We then discuss the results of holograms taken of resolution targets and particles replayed in real image mode.

## 2. DESIGN PARAMETERS

### 2.1 Design issues

A particular off-axis holographic recording can be evaluated in terms of the fidelity of the image that it reconstructs (in ideal phase-conjugate conditions). Image quality issues include the following: contrast, signal-to-noise, resolution, and the presence (or absence) of the third and higher order aberrations. If we consider the system as specialising in recording sub-millimetre sized particles, we need also consider how the particles themselves affect image fidelity. These particle characteristics include the following: shape, size, orientation (with respect to the hologram plane), light scattering issues (i.e. reflectance, transmittance and polarization) and refractive index. The morphology of an individual particle must also be expanded in the more realistic case of a mass of particles. This is because there may be important aspects exhibited by the mass of particles that influence the holographic recording and/or reconstruction processes. For example, a dense mass of particles is likely to create a significant noise background due to light scattering whereas a single particle is not. In the case of a Fresnel hologram, this same dense mass of particles creates a significant noise background from the contributions of defocused images when reconstructed<sup>14</sup>. Characteristics of a mass of particles include the following: population density, scattering, background noise and the effects of non-homogenous particles.

The design of a holographic off-axis particle recording system is further complicated by confining the particles within an aquatic medium, which is done here. The hologram is located and replayed in-air only, thus introducing a refractive index change between the recording and reconstruction volume. Other aspects of the water medium may be detrimental to the holographic recording process such as turbidity, scattering<sup>15</sup> and temperature gradient effects.

Due consideration must therefore be given to the contributions of image fidelity, particle morphology and aquatic medium issues in the system design. Within the scope of this paper, we address the principal design issues in the following subsections: reference beam geometry, third order aberrations, paraxial image sectioning replay, recording volume and illumination geometry. We discuss theoretical and experimental resolution in section 4.1 and limit our examination of particle morphology to size, shape and population density (specifically, as exhibited by plankton particles) in section 4.2.

### 2.2 Previous system design and results: an outline

Mathematical and experimental analysis of a refractive index change across a water/glass/air boundary in holographic recording and reconstruction shows that image fidelity can be improved by selecting a replay wavelength that is equal to the construction wavelength divided by the refractive index<sup>13,16-17</sup>. This wavelength compensation technique dictates that the air space between the hologram plate and the glass wall of the tank be set at one-fifth the thickness of the glass wall of the tank (the air gap condition). Our earlier work on off-axis transmission holography of plankton particles complied with

the air gap condition<sup>18</sup>. In our previous experiments, the air space was set at one millimetre, the plankton were illuminated by two diffuse beams that came from the front of the test tank and the reference beam propagated through the water to form a transmission hologram. The holograms were reconstructed in real image mode without the use of a micropositioner plate holder.

Our preliminary experimental results revealed deficiencies in the system design. At the higher particle densities (roughly  $10^1 \text{ ml}^{-1}$  for a plankton tow sample), image fidelity was degraded by the propagation of the reference beam through the water. The two object beams directed from the front of the tank could not adequately illuminate particles beyond a range of about 120 mm from the hologram plane. Most significantly, details of particle structure could not be resolved (species not identifiable). These preliminary results lead us to adopt the following design revisions:

1. The reference beam propagates in-air only so that it is unaffected by particle density.
2. The illumination beam geometry improved in order to cover a larger aquatic volume.
3. A 3-axis micropositioner plate holder used to optimize image reconstruction in order to improve particle identification<sup>19</sup>.

### 2.3 Reference beam geometry: practical considerations

If we choose a reference beam path that propagates in-air only *and* conforms to the air gap condition for wavelength compensation, two alternative geometries exist: a transmission edge-lit (waveguide) hologram or a volume (reflection) hologram. While edge-lit geometries have been shown to be feasible in display holography<sup>20</sup>, they introduce the complication of precise index matching fluids or produce spurious reflections which may degrade image quality. Within the scope of our objectives, this technique is a refinement and not further addressed here. Volume holograms are sensitive to humidity variations and processing shrinkage. This makes precise replay wavelength matching considerably more difficult, a complication that renders them inappropriate at this stage of the design.

We therefore choose to satisfy the in-air only reference beam condition as a design priority and to compromise the air gap condition. In this design, the air space is extended in order to provide clearance for an in-air only reference beam that gives transmission hologram geometry. For simplicity, we use a collimated reference source (and consequently, a collimated reconstruction source).

### 2.4 Third order aberrations: spherical aberration and astigmatism

Mathematical analysis of an air/glass/water boundary shows that paraxial subjects recorded in water exhibit significant spherical aberration when replayed in air. Similarly, subjects not located along the optic axis exhibit significant astigmatism<sup>13</sup>. Within the scope of this paper, we consider spherical aberration and astigmatism as critical "aberration indicators" to the system design, as will become evident. The refractive index mismatch gives rise to spherical aberration as the hologram aperture increases. This is clearly because a larger reconstruction area (at the hologram plate) increases the extent of the marginal reconstruction rays. The refractive index mismatch also gives rise to astigmatism as the hologram field of view increases. Clearly, this is a result of (particle) images further from the optic axis being reconstructed.

Geometric expressions have been derived for the magnitude of longitudinal spherical aberration (LSA) and astigmatic difference, respectively, that take the forms<sup>13</sup>

$$S_L = \frac{z_w}{\mu\eta_{wa}} \left[ 1 - f(\mu\eta_{wa})^{1/2} \right] + \frac{z_g \eta_{wg}}{\mu\eta_{wa}} \left( 1 - \frac{f(\mu\eta_{wa})^{1/2}}{f(\eta_{wg})^{1/2}} \right) + \frac{z_a \eta_{wa}}{\mu\eta_{wa}} \left( 1 - \frac{f(\mu\eta_{wa})^{1/2}}{f(\eta_{wa})^{1/2}} \right) \quad (1)$$

$$A_d = \frac{1}{\mu\eta_{wa} \sin\theta} \left[ z_w \tan\theta(1 - f(\mu\eta_{wa})) + \frac{z_g \eta_{wg} \tan\theta}{f(\eta_{wg})^{1/2}} \left( 1 - \frac{f(\mu\eta_{wa})}{f(\eta_{wg})} \right) + \frac{z_a \eta_{wa} \tan\theta}{f(\eta_{wa})^{1/2}} \left( 1 - \frac{f(\mu\eta_{wa})}{f(\eta_{wa})} \right) \right] \quad (2)$$

where  $\lambda_c$  = the hologram construction wavelength,  $\lambda_r$  = the hologram replay wavelength,  $\mu = \lambda_c / \lambda_r$ ,  $\theta$  is the angle subtended by the marginal ray at the object point in water,  $z_a$  is the axial air space distance,  $z_w$  is the axial distance to the far subject point in water and  $z_g$  is the window thickness  $n_w$  is the refractive index of water,  $n_a$  is the refractive index of air,  $n_g$  is the refractive index of the (glass) window,  $\eta_{wa} \equiv n_w / n_a$ ,  $\eta_{wg} \equiv n_w / n_g$ , and  $f(x) = 1 + (1-x^2)\tan^2\theta_w$  is used as an abbreviated notation.

Figures 1 and 2 present plots of predicted astigmatic difference and LSA as a function of field angle and marginal ray extent, respectively, for reconstructed image points at incremental values of  $z_w$ . Observe, from figure 1, that the severity of astigmatic difference increases rapidly with field-of-view for values of  $z_w$ . Similarly, from figure 2, observe that the severity of LSA increases rapidly with marginal ray extent for values of  $z_w$ . One can reasonably predict that the combination of astigmatism and spherical aberration seriously degrades image fidelity for a field-of-view and marginal ray extent beyond about 4 degrees (at other than small values of  $z_w$ ). Using LSA and astigmatic difference as the key "aberration indicators" for particle positions on and off the optic axis, respectively, it is evident that without some form of correction only narrow field recording (or replay) conditions are suitable in order to resolve sub-millimetre particle images.

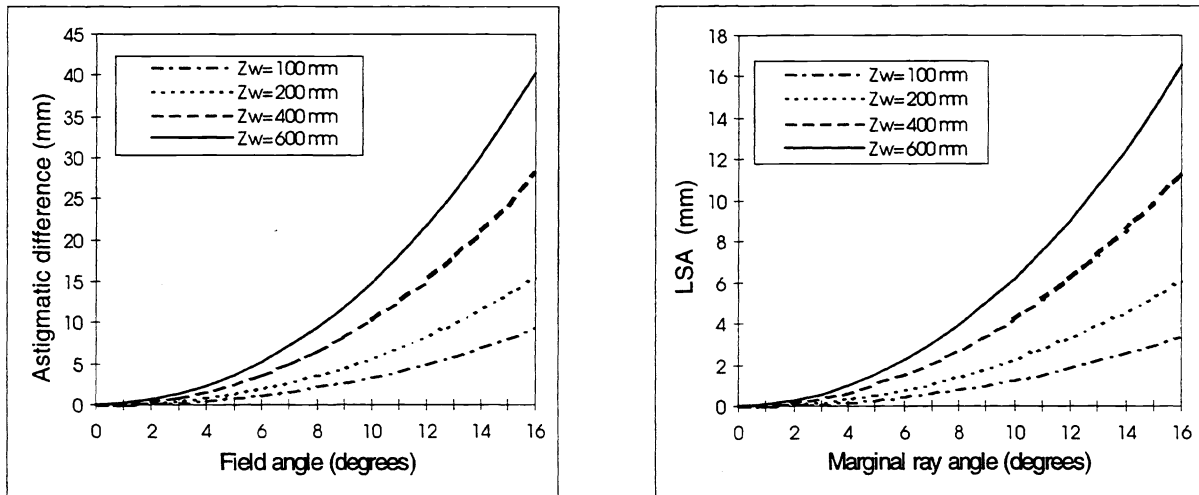


**Figure 1** (left) Astigmatic difference as a function of field angle. **Figure 2** (right) Longitudinal spherical aberration as a function of marginal ray angle. Both figures show plots for far particle distances in water where  $z_g = 5$  mm,  $z_a = 120$  mm and  $\lambda_c = \lambda_r = 694$  nm.

### 2.5 Paraxial image sectioning replay

The narrow field conditions necessary for stigmatic imagery seem, at first glance, to be in direct conflict to a large volume recording. In other words, if we severely limit the extent of the marginal rays *and* only consider image points that lie on or near to the optic axis, the usable volume of the hologram seems very small indeed. However, if we sacrifice most of the parallax information inherent in the holographic recording, we can re-consider the same problem in different terms.

Consider, for the moment, an individual particle within the recording volume and the area of reference beam illumination at the hologram plate. If the particle has a principal ray normal to the hologram plane that lies within the reference beam area at the hologram plate, then the particle image will necessarily have a principal ray normal to the hologram plane that can be reconstructed by the hologram (in phase-conjugate conditions). Thus, each particle that satisfies the above criterion can be considered in the paraxial sense only, which simplifies the analysis to first order theory. In other words, each paraxial reconstruction ray (approximately normal to the hologram plane) corresponds to a point at the hologram plate. Consider now the summation of all these paraxial image points. Thus defined, the usable volume of the hologram is larger than what, at first, seemed rather small. In fact, it takes the shape of a cylinder extruded from the reference beam area at the hologram plate. In practice, one can not expect to reconstruct a recognisable image of even a very small particle on the basis of a single paraxial ray. Recall, however, our observation of the "aberration indicators" from the previous section, namely, about 4 degrees of acceptable marginal ray extent for sub-millimeter particle size.

In another sense, replay conditions that are thus severely restricted limit the parallax information inherent in the holographic recording. That is, *parallax information is discarded*. This means that the hologram plate is reconstructed in sections that correspond their paraxial image counterparts. The hologram particle images can be replayed as two-dimensional planar sections normal to the hologram plate and yet retain three-dimensional spatial information.

## 2.6 Recording volume

Assume that a recording volume of particles is isotropic; therefore, the dimensions of the volume can, for the moment, be considered arbitrary. What is clearly important in the system design is maximizing the recording volume. Now, if we consider the volume as a severely limited field angle cylinder, or "water core", the recording volume can be defined by the reference beam area at the hologram plane and the distance of the far particle,  $z_w$ . For an elliptical reference beam profile at the hologram plane, the recording (or replay) volume of the "water core",  $V_R$ , can be given simply as

$$V_R = (\pi ab) z_w \quad (3)$$

where  $a$  is the minimum radius of the reference beam profile on the hologram plane,  $b$  is the maximum radius of the reference beam profile on the hologram plane, and  $z_w$  is distance to the far particle.

## 2.7 Illumination geometry

From equation 3, it is evident that as  $z_w$  increases so does  $V_R$ . If we hold the reference beam area at the hologram plane constant (due to the practical limitation of plate size), this relationship puts the onus on an illumination geometry that can give sufficiently large values of  $z_w$ . In the case of a front-lit geometry, this simply means that the far particle at  $z_w$  must reflect enough light during the exposure for image formation at the hologram plate. Recall, however, that front lighting tends to adequately illuminate only the plankton particles near the hologram plane ( $z_w = \sim 120$  mm). Also, as particle densities increase, scattering effects reduce the distance at which particles can be resolved (this is broadly analogous to the ineffectiveness of headlights to improve visibility in dense fog).

An alternative illumination geometry for off-axis particle holography is the use of subject back lighting<sup>12</sup>. In this case, it is reasonable to expect that the paraxial reconstructed subject beam is higher in intensity than an individual particle for points viewed along the optic axis. This is not necessarily true when one considers particle morphology, as is evident in the case of bubbles, which exhibit the characteristics of negative lenslets when recorded in water, but which reconstruct a apparent focus (behind the bubble) in air that is brighter than the subject beam illuminating them. Experiments using a negative USAF 1951 resolution target at the rear of the tank confirmed a bright background noise level along the optic axis--"weak" particles could be seen only when viewed at points off the optic axis.

The illumination geometry we devise is a side lighting array that traverses the length of either side of the tank (figure 3). The array is produced by a series of plate glass beamsplitters, each surface reflecting approximately 10 percent of the light incident upon it at 45 degrees. The light from each beamsplitter is directed towards the tank normal to the glass wall. The illumination beams originate from the end opposite the hologram plane. This design thus provides more light energy to particles at the farther distances than to particles closer to hologram plane. The recording volume is therefore closer to a state of balanced illumination relative to the hologram plate than in the front-lit case. We expect that this design will prove more effective than our preliminary front-lit version for maximizing  $z_w$  at the higher particle densities.

### 3. SYSTEM CONFIGURATION

#### 3.1 Off-axis holographic set-up

Figure 3 depicts the experimental off-axis holographic set-up. A ruby laser (Lumonics 2000) was operated with the following characteristics: Q-switched, 750 mJ output energy at 40 ns pulse duration; TEM<sub>00</sub> at 694 nm output wavelength; etalon tuned to provide coherence length greater than 1 meter. Light reflected from the 60/40 beamsplitter forms one path of an arrayed subject illumination along the left side of the test tank. Approximately 10 percent of the light transmitted through the 60/40 beamsplitter is reflected by an optical flat beamsplitter as the reference beam. The reference beam is expanded, spatially filtered (focused energy levels are below air breakdown threshold) and collimated. Light transmitted through the optical flat beamsplitter forms a second path of an arrayed illumination along the right side of the test tank. The subject beams from either side of the tank are interlaced (not shown in figure 3) in order to provide greater illumination continuity. For this geometry we set  $\theta_{ref} = 60$  degrees,  $z_a = 120$  mm,  $z_w = 600$  mm,  $a = 30$  mm and  $b = 60$  mm. This yields (from equation 3)  $V_R = 3,390 \text{ cm}^3$  (assuming, for the moment, that  $z_w$  is within resolution tolerances).

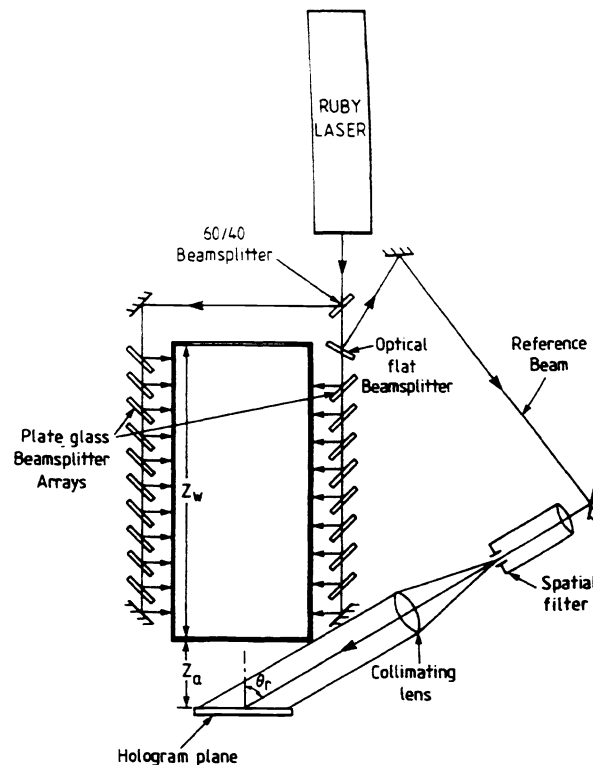


Figure 3 The off-axis recording set-up.

## 4. RESULTS

### 4.1 Resolution.

The resolution of a holographic diffraction limited system (without allowances for laser speckle) can be given as

$$R = D / (1.22\lambda z) \quad (4)$$

where  $D$  is the aperture of the hologram,  $\lambda$  is the wavelength of laser light and  $z$  is the distance of the subject normal to the hologram plane (if all unit values are given in millimetres, then the resolution is given in line pairs per millimetre).

A hologram was taken of a USAF 1951 target at the farthest distance in water from the hologram plane ( $z_w = 600$  mm) to test the resolution of the experimental off-axis set-up. The target was oriented parallel to the recording plate (and to the parallel illumination rays incident upon it). As a consequence of this oblique illumination angle, the light rays reflected from the target surface (covered by a transparent waterproof coating) dominated the light rays transmitted to the target. To overcome this problem, two diffuser panels of opal Perspex™ were added to the sides of the tank. An amplitude hologram was processed using a 50 percent molar pyrogallol / ascorbic acid developer and replayed in real image mode using the 647 nm line of a krypton-ion laser. The hologram was reconstructed in real image mode using a computer controlled 3-axis micropositioner plate holder as an aid to optimising the plane of best focus (by visual inspection of the image). The holographic real image was relayed by newvicon camera (equipped with a reverse mounted Nikon 50 mm lens) to a high resolution CRT display.

For  $D = 45$  mm (centred about the normal to the optic axis) we obtain the theoretical resolution limit for an incoherent source,  $R = 95$  lp/mm. Reducing by a factor of 2.5 to account for degradation due to laser speckle<sup>21</sup> this limit becomes  $R = 38$  lp/mm. We observed the experimental value  $R = 7$  lp/mm (USAF 1951 target: group 2, between elements 5 and 6) or approximately  $140 \mu\text{m}$  (figure 4). While this value is substantially below the theoretical limit (albeit for air-only recording and replay) it is clearly adequate to resolve sub-millimetre structure.

### 4.2 Particle morphology: plankton

A series of ten holograms were taken of preserved marine plankton (collected from the Clyde Sea in July 1995, fixed in Lugol's iodine). The plankton particles ranged in size from approximately  $20 \mu\text{m}$  to several millimetres. The shapes of the particles were specific to the species (for example, a *Calanoid copepod* as shown in figure 5).

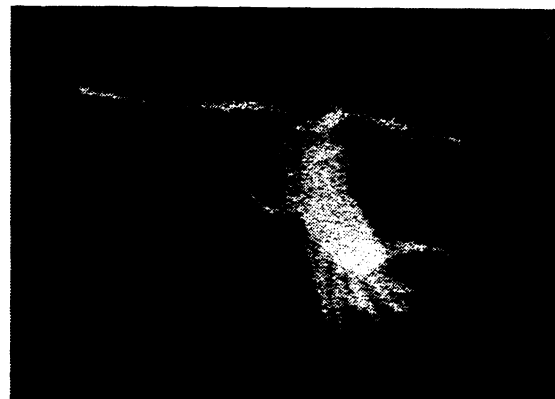
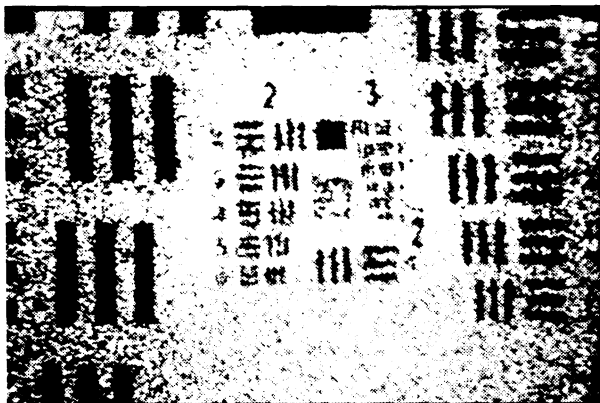


**Figure 4** (left) Photograph of a reconstructed USAF 1951 target ( $z_w = 600$  mm) taken from CRT monitor. **Figure 5** (right) Photograph taken of *Calanoid copepods* plankton (approximately 2 mm in length) reconstructed from an off-axis hologram.

The test tank was initially filled with 36,000 cm<sup>3</sup> of de-ionized water. Incremental doses of the particles were added after each exposure. Hence, the plankton particle levels in the tank represented a cumulative increase in population density. In order to reduce settling and help maintain a homogenous density within the tank, a magnetic stirring device was added to the floor of the tank. The two diffuser panels used to illuminate the resolution target were removed to reduce scattering effects. The holograms were processed as in section 4.1. The holograms were reconstructed in real image mode using the micropositioner plate holder as in section 4.1, and observed at best focus on a finely-ground glass screen mounted on computer controlled micropositioner.

Before each exposure, a one millilitre sample was taken from the tank for conventional microscope analysis. From each sample, 40 random fields of view were scanned and the results categorised in terms of particle size, classification, and count<sup>14</sup>. For  $V_R = 3,390 \text{ cm}^3$ , a scaled estimate based on the 1 ml samples taken for microscopic analysis yields a total of  $3.8 \times 10^4$  particles at the low population density sample and  $1.2 \times 10^6$  particles at the high population density sample. These values include non-identifiable particles (in the 20 - 200  $\mu\text{m}$  size range) that represent approximately 60 percent of the total population for the low density sample and approximately 18 percent of the total population for the high density sample.

Holographic particle counts were observed for 1 cm<sup>3</sup> volume (1 cm x 1 cm x 1 cm) samples. Each hologram was sampled at five incremental axial distances (at approximately 10 cm intervals), from  $z_w = 2.5 - 3.5 \text{ cm}$  to  $z_w = 45.5 - 46.5 \text{ cm}$ . Taking the average of the five sample distances, for  $V_R = 3,390 \text{ cm}^3$ , the holographic analysis yields a total of  $2.7 \times 10^3$  particles at the low population density hologram and  $5.6 \times 10^4$  particles at the high population density hologram. We note here that the holographic data to date does not include information on the percentage of unidentified particles.

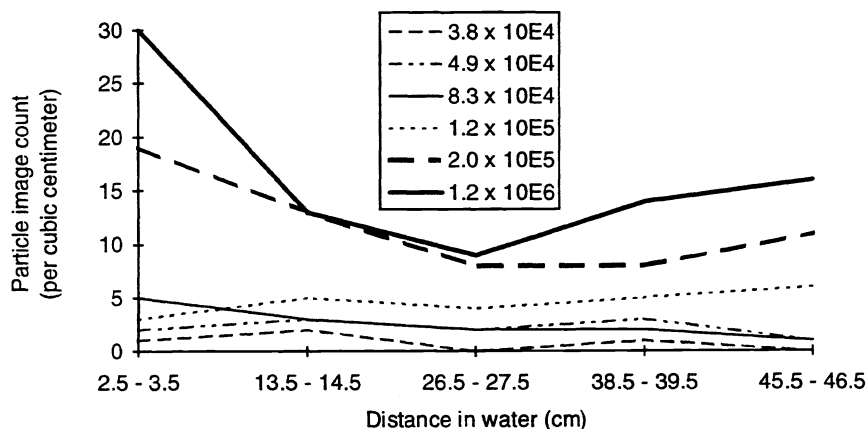


**Figure 6** Holographic particle counts at selected population densities ( $V_R = 3,390 \text{ cm}^3$ ) as a function of distance in water. The densities were determined by scaled estimate (of a 1 ml sample) using conventional microscopic sampling methods.

Figure 6 presents a graph of hologram particle image count as a function of water distance for selected population densities (determined by scaled estimate of conventional microscopic sampling methods). Most test holograms exhibit a drop in particle count near the midpoint of test tank. This may be due to a vortex effect of the magnetic stir bar, which was located at the center of the tank floor. Alternatively, it may be a result of deficient subject illumination within the central depth planes sampled.

The particle counts made by real image reconstruction from off-axis holograms show a strong correlation to the microscope counts if we consider the larger particles only (greater than approximately 600  $\mu\text{m}$ , classified as macro-zooplankton). Given the limiting system resolution of 7 lp/mm in ideal aquatic conditions (e.g. negligible turbulence gradients, clear water) it seems reasonable for the moment to operate under this assumption.

An encouraging result of the holographic sampling is that, at even the highest population density, particle counts do not drastically decrease with an increase in  $z_w$  (indeed, in some holograms the counts exhibit a peculiar rise). This leads us to believe that the illumination scheme works within our approach of a limited field angle "water core" design. It also leads us to believe that the system may, within resolution limits, be scaled up to greater values of  $z_w$  and therefore larger test volumes.

## 5. CONCLUSIONS

We have described an off-axis transmission holographic design for recording (and replaying) aquatic particles. We have recorded particle sizes (sub-millimetre to several millimetres) and population density limits (ranging from  $1.1 \times 10^1$  to  $3.6 \times 10^2$  per ml for a plankton tow sample) that are beyond the predicted theoretical values for in-line Fraunhofer holography. We have also provided spatial information (from the five sampled planes in section 4.2) within a large recording volume,  $V_R = 3,390 \text{ cm}^3$ .

Paraxial image sectioning replay that restricts the parallax information of the reconstructed image is acceptable for our purposes because our exploitation of the design is to identify and spatially map particles.

A precise Cartesian co-ordinate plot of particles is not yet available for the off-axis holograms described here. (The authors have thus far implemented a replay system to plot particle points in 3-space for in-line holograms, PHOENIX, at Brunel University).

The system design can in theory be scaled upwards to record and replay larger volumes (provided that the particles can be resolved) by either increasing the axial illumination distance or the size of the recording area at the hologram plate. Figure 7 depicts a concept field camera.

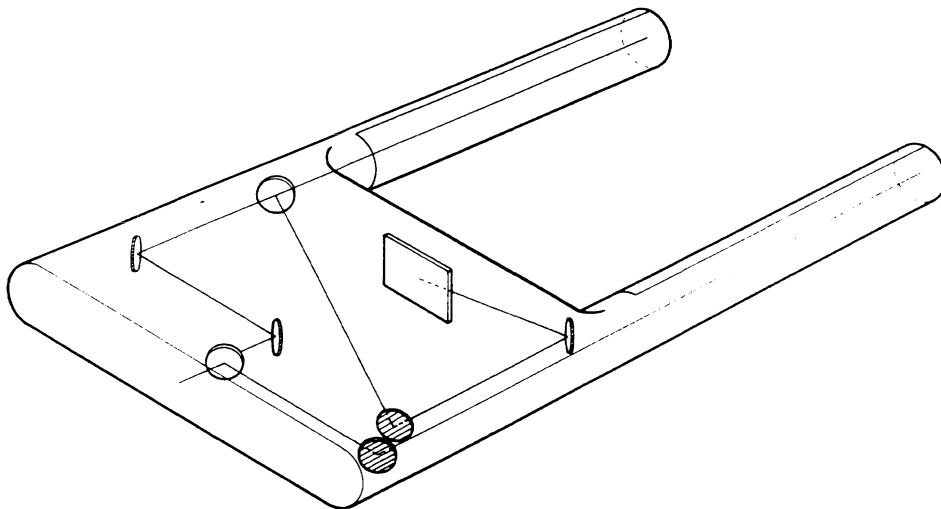


**Figure 7** An off-axis holographic concept field camera.

## ACKNOWLEDGEMENTS

This work was carried out at the Laser Laboratories, Department of Engineering, University of Aberdeen. Invaluable assistance was given by Elizabeth Foster and John Polanski. This work was supported in part by a grant from the University Court of the University of Aberdeen (for E. Krantz) and by a grant from the National Environmental Research Council of Great Britain (NERC).

## REFERENCES

1. Pedros-Alio, C. & Brock, T.D. (1983) "The importance of attachment to particles for planktonic bacteria." *Arch. Hydrobiol.* **98**: 354-379
2. Taylor, A.H., Harris, J.R.W. & Aiken, J. (1986) "The interaction of physical and biological processes in a model of the vertical distribution of phytoplankton under stratification." *Marine Interfaces Ecohydrodynamics* (ed. by J.C.J. Nihoul), Elsevier, Amsterdam, Oxford, New York, Tokyo.
3. Alldredge, A.L. & Silver, M.W. (1988) "Characteristics, dynamics and significance of marine snow." *Prog. Oceanogr.* **20**: 41-82
4. Rogerson, A. & Laybourn-Parry, J. (1992) "Aggregate dwelling protozooplankton communities in estuaries." *Arch. Hydrobiol.* **4**: 411-422
5. Lampitt, R., Hillier, W.R. & Challenor, P.G. (1993) "Seasonal and diel variation in the open ocean concentration of marine snow aggregates." *Nature*, **362**: 737-739
6. Yamamoto, *et al.*, (1995) "A laser light scattering *in situ* system for counting aggregates in blood platelet aggregation." *Meas. Sci. Technol.*, **6**: 174-180
7. Hobson, P.R. (1988) "Precision co-ordinate measurements using holographic recording." *J. Phys. E.: Sci. Inst.*, **21**: 138-145
8. Carder, K.L. *et al.*, (1982) "In situ holographic measurements of the sizes and settling of oceanic particulates." *J. Geophys. Res.*, **87**: 5681-5685
9. Knox, C., (1966) "Holographic microscopy as a technique for recording dynamic microscope subjects." *Science*, **153**: 989-990
10. Hobson, P.R., Krantz, E.P., Watson, J., Lampitt, R.S., Rogerson, A., "The study of suspended particles in aquatic systems using underwater hologrammetry" presented at conference of Underwater Optics, (October 1995) Kettering, U.K. Organised by The Optics Group of the Applied Optics Division of the Institute of Physics.
11. van de Hulst, H. C., (1957) "Light Scattering by Small Particles." (London: Chapman & Hall, Ltd.) pp. 103-113
12. Santangelo, P.J. & Sojka, P.E. (1994) "Holographic Particle Diagnostics." *Prog. Energy Sci.*, **19**: 587-603
13. Kilpatrick, J.M. & Watson, J. (1994) "Precision replay of underwater holograms." *Meas. Sci. Tech.*, **5**: 716-725
14. Krantz, E.P., Watson, J., Hobson, P.R., Lampitt, R.S., Rogerson, A. (1996) "In situ off-axis holography of marine plankton." To appear in Practical Holography X, *SPIE proc. vol. 2652* (In press).
15. Bohren, C.F. and Huffman, D.R., (1983) "Absorption and scattering of light by small particles." (New York: J. Wiley & Sons) pp.425-429.
16. Kilpatrick, J.M. & Watson, J. (1988) "Underwater hologrammetry: aberrations in the real image of an underwater object when replayed in air." *J. Phys. D.: Appl. Phys.* **21**: 1701-1705
17. Kilpatrick, J.M. & Watson, J. (1993) "Underwater hologrammetry: reduction of aberrations by index compensation." *Appl. Phys.* **26**: 177-182
18. Watson, J., Hobson, P.R., Krantz, E.P., Lampitt, R.S., Rogerson, A. (1995) "Holographic mensuration of suspended particles in aquatic systems." in Applications of Optical Holography, Toshio Honda, Editor, *SPIE proc. vol. 2577* 191-199.
19. Ross, G. & Watson, J., (1992) "Effects of misalignment on real image holographic measurement." in Holographics international, *SPIE proc. vol. 1732* 198-208
20. Benton, S.A., Birner, S.M. & Shirakura, A. (1990) "Edge-lit rainbow holograms." *SPIE proc. vol. 1212 Prac. Holo. IV*, 149-157
21. Kilpatrick, J.M., (1991) "An evaluation of optical aberrations in underwater hologrammetry." PhD thesis (University of Aberdeen Library) p.18